

# Simulation Validation of the Analytical Model of Differential Inductive Servo Sensor for Imaging Signal Generation and Measurement Applications

Abdulwahab Deji<sup>1</sup>, Bashir Esima Musa<sup>2</sup>

<sup>1</sup>Department of Electrical and Computer/Telecommunication Engineering, Waidsum University, Malaysia.

<sup>2</sup>Department of Mechanical and Production Engineering, University of Benin, Nigeria

## Abstract

This paper explores the utility of the seesaw model sensor apparently giving a differential output in a differential manner, which validates one of the major findings of this research using simulation techniques. In this article, simulation is carried out of the designed mathematical model and its necessary derivations for frequency, frequency hysteresis, sensing voltage, magnetic field strength, resonant frequency, mass of bar and mass of target object and the current excitation responses also obtained. Furthermore, the linearity issues of the transducer response curve are addressed for an application scenario of using an inductor with 3R resistor in a differential manner. The parameter of interest is displacement of the core bringing about changes in inductance. Displacement makes the differential inductor to oscillate and undergo changes in differential style. Other parameters of interest such range, frequency, inward output voltage, outward output voltage were explored and results obtained validated the analytical modelling from mathematical derivations in recent literature.

**Keywords:** frequency, frequency hysteresis, sensing voltage, magnetic field strength, resonant frequency, mass of bar and mass of target object and the current excitation, range, frequency, inward output voltage, outward output voltage.

## 1. INTRODUCTION

Transducers and sensors are undoubtedly found their niche applications in today's instrumentation and telecommunication engineering and their circuits are deployed comprehensively for measurement, derivation of imaging signals for biomedical applications as well as control used in research and development corridor and industrial system engineering applications. However, these sensors naturally produce analog output signals which are interfaced with processor circuits such as microprocessor and other electronic circuits. They are used to modify and producer the output signal in a usable format by the next stages of the processing concepts. Deji, A., Khan, S., Habaebi, H.M., Musa. O.S. (2024, Deji A., , Sheroz K., Musse M.A., (Jan-Feb 2024), Deji A., Sheroz K., Musse M.A., (December 2023 and Deji A., Sheroz K., Musse M.A., (December 2023). Furthermore, the linearity issues of the transducer response curve are addressed for an application scenario of using an inductor with 3R resistor in a differential

manner. This is displayed using magnetization and demagnetization techniques together with the charging and discharging concept of the voltage. However, the parameter of interest is displacement of the core bringing about changes in inductance and hence output frequency, voltage in form of sensed parameter or being converted from the parameter sensed is harnessed as an image signal from the biomedical application. Displacement makes the differential inductor to oscillate and undergo changes in differential style. Other parameters of interest such range, frequency, inward output voltage, outward output voltage and the sweeping voltage which are reported in this paper. Deji A., Sheroz K, Musse M.A, Jalel C. (August 2014), Deji A., Sheroz K, Musse M.A, Jalel C. (2011) Abdulwahab D., (2011), Abdulwahab D.,(2016), Deji A., Sherifah OM., 2023, Elfaki Ahamed, O.M.H., Musa O.S, Deji A. 2023. The simulation of the differential sensory circuit used for this verification of how mechanical vibrations (machine vibrations and oscillation) sensed are converted to useful electrical signal obtained from the mathematical concept published and in literature is simulated as shown in Figure 1. Hence, a servo sensor for accurate position and angular measurement is obtained.

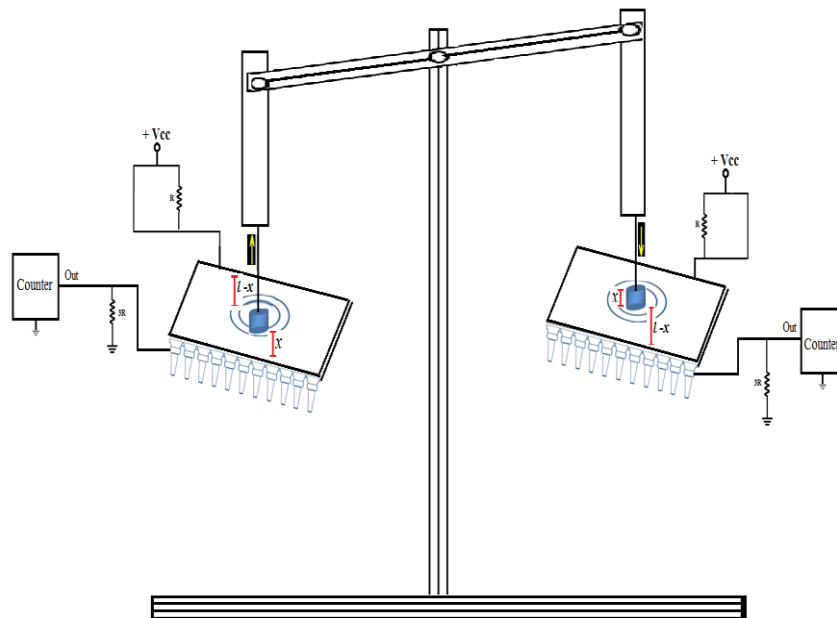


**Figure 1: Simulation of Differential Sensory Circuit Prototype**

The linearization circuit, duty cycle, magnetization/demagnetization and charging/discharging techniques are shown in the work. The accuracy of the designed circuit emanating from simulation results are presented and discussed. This research also identifies regions on a transducer response curve using mathematical analysis to compensate for system's inaccuracy of a transducer curve. Deji A., Sheroz K., Musse M.A., (Jan-Feb 2024).

## 2. CIRCUIT DESIGN SIMULATION

The results obtained confirm the mathematical derivation plots with the simulation. Figure 1 is the result of simulation of both circuits; the right and the left one using the same assumption adopted in the calculations in Deji A., Sheroz K., Musse M.A., (December 2023 and Deji A., Sheroz K., Musse M.A., (December 2023). The frequency output of the left side and the core displacement from the right hand measurement vice versa.

The simulated output result obtained is as a result of variations in inductance of the circuit. These outputs consist of voltage, frequencies, duty cycle, which are all shown to be proportional to the physical parameter of interest such as displacement, speed, range of the oscillating bar, number of oscillations, acceleration, angularity, force, pressure. Deji A., Hanifah A.M., Sherifah O.M., (December 2023), D. Abdulwahab et al., D. Abdulwahab, S. Khan, J. Chebil and A. H. M. Z. Alam 2011, Khan S., A. Deji, A.H.M Zahirul, J. Chebil, M.M Shobani, A.M Noreha. (September 2012)

Simulation is done in this work using Orcad Pspice, Multisim, and Simulink. The circuit is similar to differential resistor. However, in this case, inductive variation is used in providing the output signal. A notable result is the frequency output against the change in inductance,  $L_1$ . As mentioned in in Deji A., Sheroz K., Musse M.A., (December 2023 and Deji A., Sheroz K., Musse M.A., (December 2023, in the first arm of the seesaw, as the displacement is increased, the inductance is also increased. Here,  $L_1$  is varied as the parameter that is inductance value of  $L_1$  increases. The value of  $L_1$  has been swept incrementally. The schematic circuit diagram of the first arm simulation are shown in Figure 2 (a) and (b)

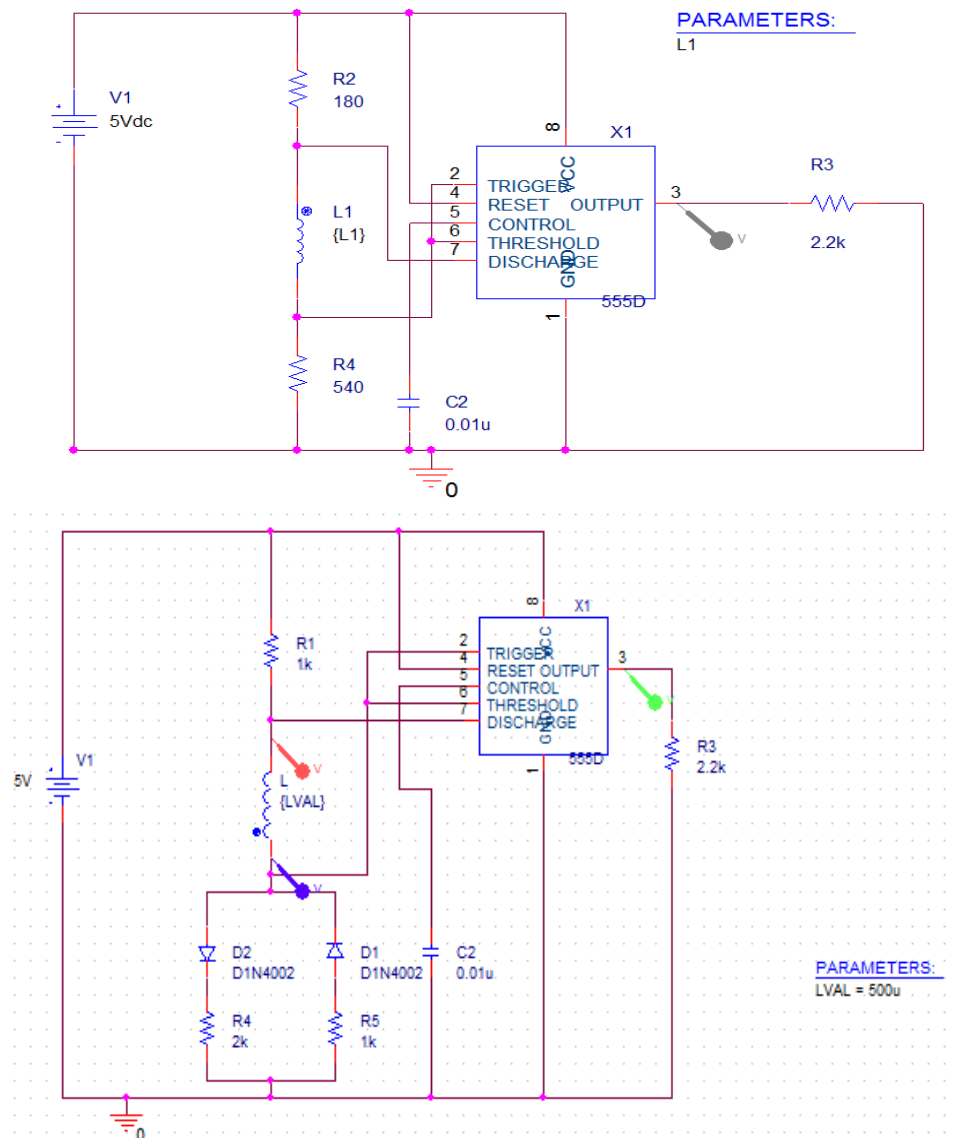


Figure 2 (a) Schematic of the first arm Simulation of the seesaw (b) Schematic of the L3R Simulation of the seesaw

Figure 2 (b) shows the schematic of desired proposed design. In this case, we use timer as trigger pulse of changing state whenever the value of inductance is swept. With this, we can observe the differential manner of seesaw overhanging bar mechanism by sweeping the value of inductance parameter. In the first part, the inductance parameter is swept from low to high value while in the second part; the inductance parameter is swept from high to low value. The simulation setting is shown in Figure 3.

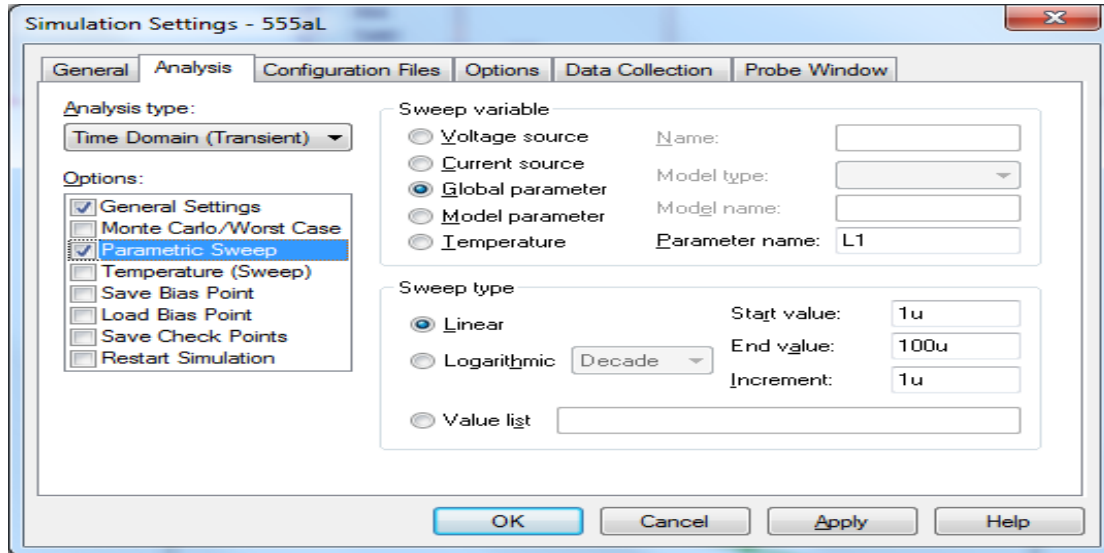


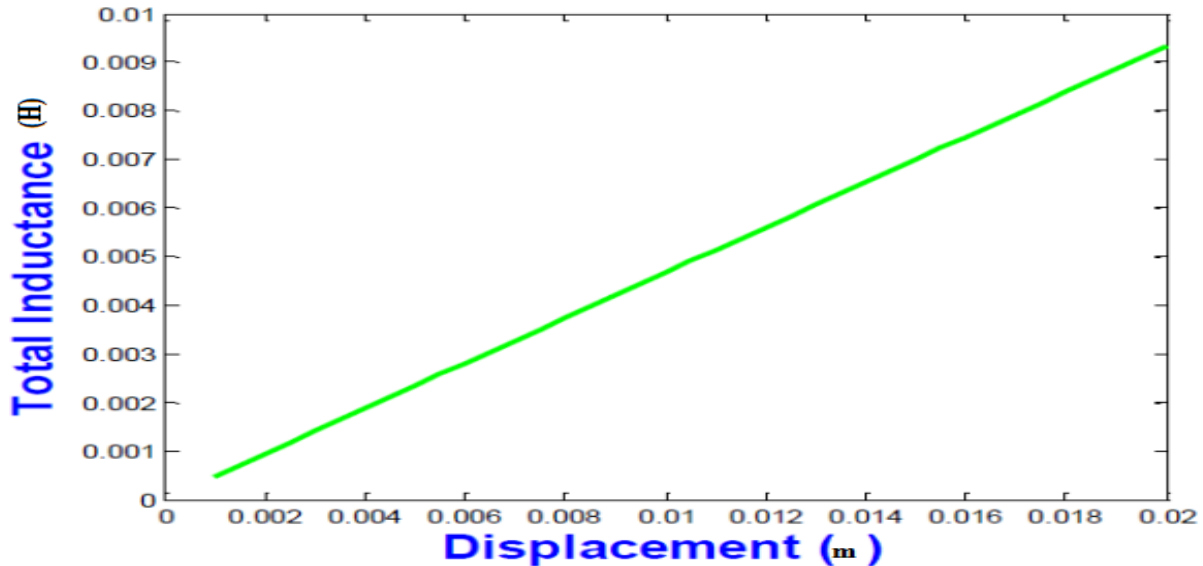
Figure 3: The simulation setting using 555 Timer as processor

### 3. SIMULATION RESULTS AND ANALYSIS

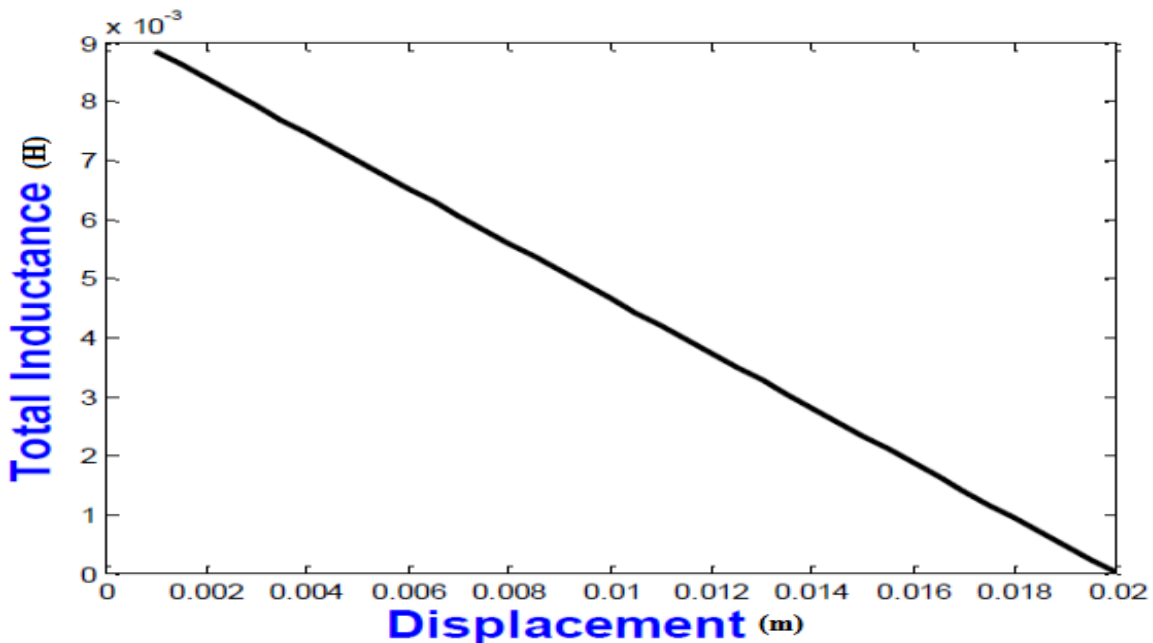
The range of the bar affects the frequency of oscillation and hence the simulated results. The longer the bar, the more easily it oscillates producing rapid changes in inductance as a result the magnetic core displacement in the coil geometry. This affect the overall output results from both arms as in and out motion is produced simultaneously as a result of the oscillation. Therefore, factors such as range, frequency of oscillation are necessary input parameter to be taken care of in order to obtain the desired output. The shorter the length of the bar, the lower the frequency of oscillation and hence the smaller are the inductive changes, making every other output signal such smaller than it should be. To make sensor perform favorably, a considerable length of the convulsion bar is chosen and also the range of both the right and left arms have been carefully modeled and simulated.

Figure 4 is the result of simulation of both circuits the right and the left one using the same assumption that was used in the derivation. The green line represents inductance and the frequency output of the left arm and the black one is for the circuit in the right hand arm as a measure of the core displacement. This output result confirms the derivation results obtained earlier for frequency Deji A., Sheroz K., Musse M.A., (December 2023 and Deji A., Sheroz K., Musse M.A., (December 2023. The right arm of the position sensor configuration has an output frequency which increases as the inductance increases while the left arm of the designed sensor's frequency decreases as the inductance increases hence producing the desired differential output in a differential as a huge improvement to Ezzat 2011, Muhammed S.S., 2012. From Figure 4 (b), the simulated circuit is designed to address linearity issues. This is ensured using diode alongside with RL3R for characteristic linearization. This produces an output inductance, which is linearly proportional to the displacement of the magnetic core in the coil geometrical topology. These improvements have been shown in Figure 4 (a)-(b). In the result presented before, the inductance of both arm of the designed position sensor increases linearly with increase in displacement from the right arm as

shown in Figure 4 (a) and decreases linearly with increase in displacement from the left arm as shown in Figure 4 (b)



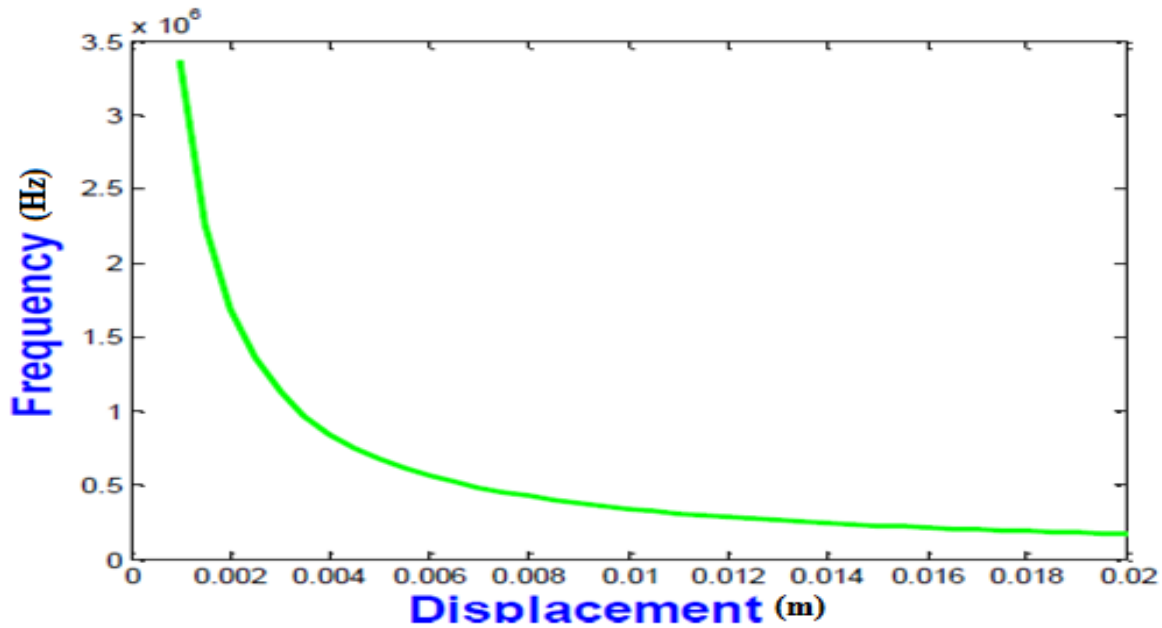
(a)



(b)

**Figure.1 (a) The Linearized Inductance of the right arm Coil against displacement (b) The Linearized Inductance of the left arm Coil against displacement**

For the inductance of the right arm coil, the simulated frequency output from timer is given in Figure 5 (a). This shows an exponential response. The frequency in this case decreases exponentially as the displacement increases. The frequency of the left arm coil against displacement is shown in Figure 5 (b). This shows an exponential increment in the stimulated frequency confirming the derivation plot and analysis in Deji A., Sheroz K., Musse M.A., (December 2023 and Deji A., Sheroz K., Musse M.A., (December 2023).



(a)

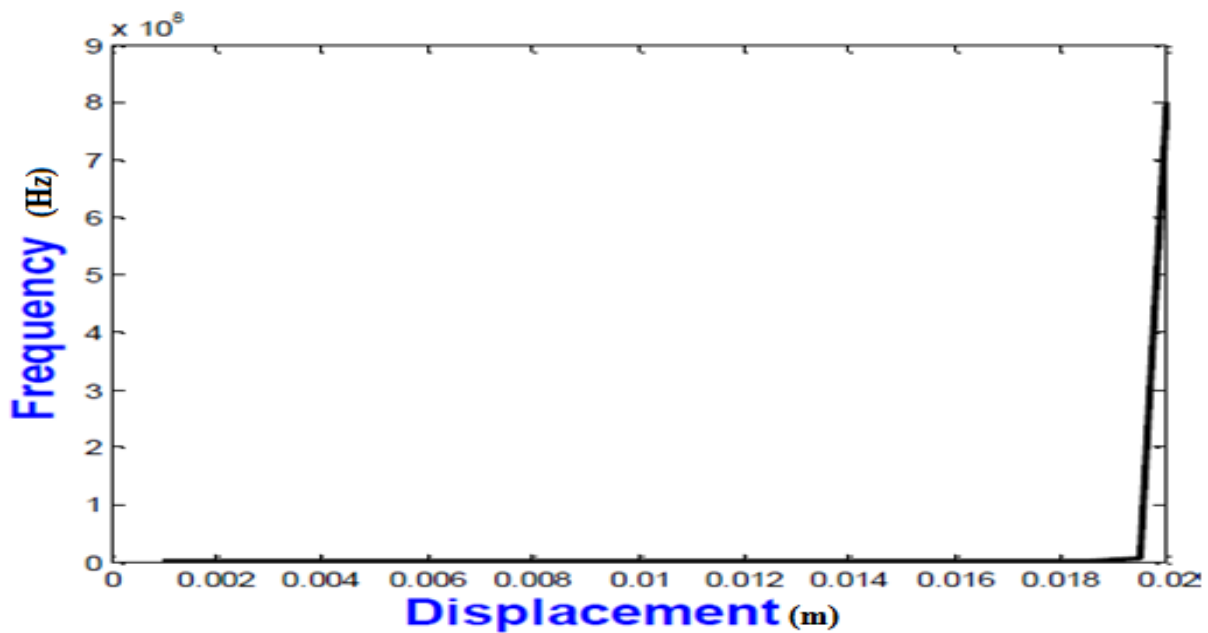
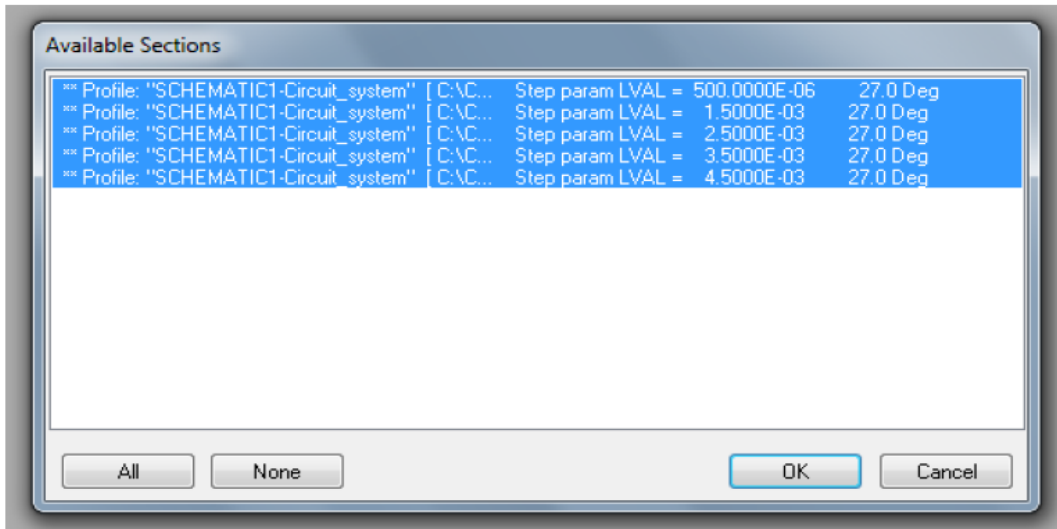


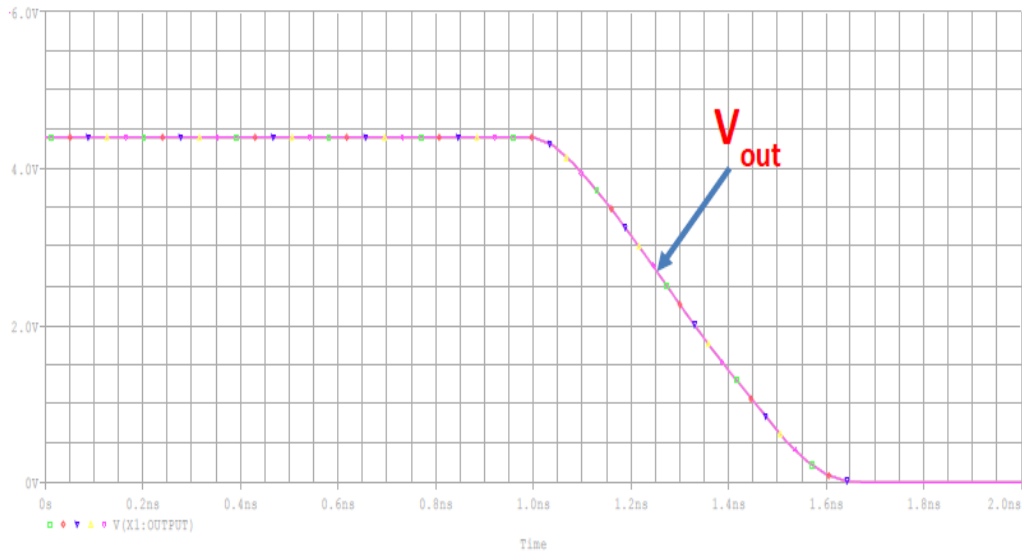
**Figure: 2 (a) The change in frequency of the right arm Coil against displacement (b) The change in frequency of the left arm Coil against displacement**

#### **4. THE SWEEPING OF THE INDUCTANCE VALUE FROM LOW TO HIGH AS THE CORE IS DISPLACED IN SIMULATIONS**

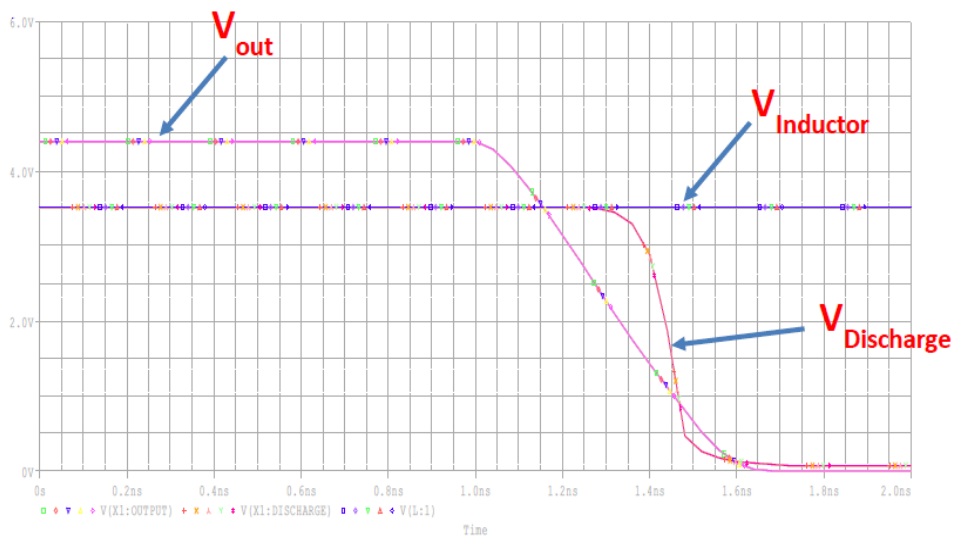
The inductance of the circuit is swept from low value to high value for the right arm coil and is given in Figure 6 (a-c), while that of the left arm coil is swept also from low to high value is shown in Figure 7 (a-c). Their corresponding sweeping voltages for the right arm for output voltage, inductive voltage and discharge voltages are shown in Figure 6 (b)-(c) and for the left arm shown in Figure 7 (b)-(c).



(a)



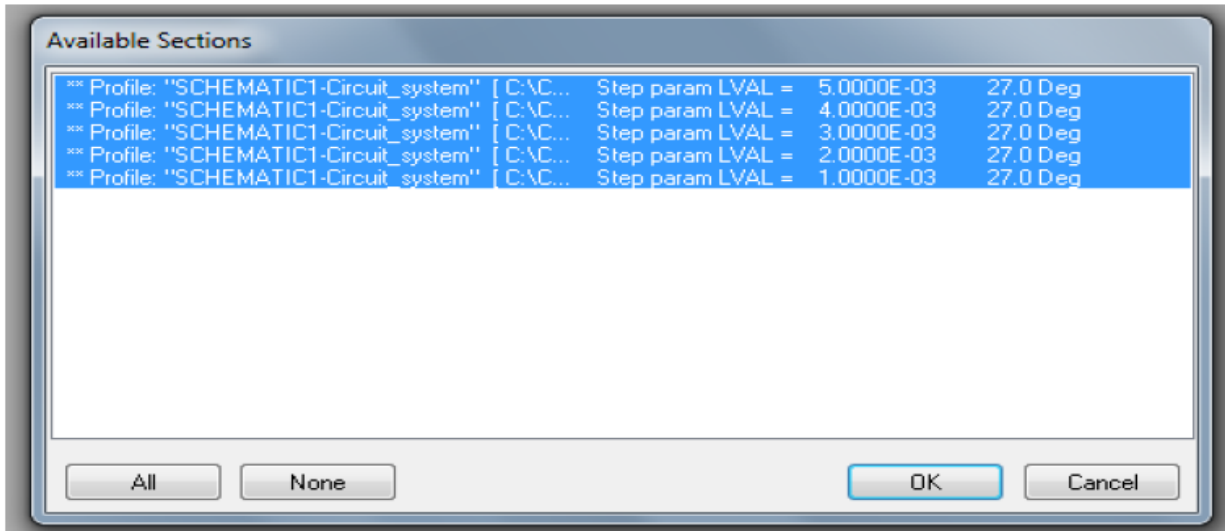
(b)



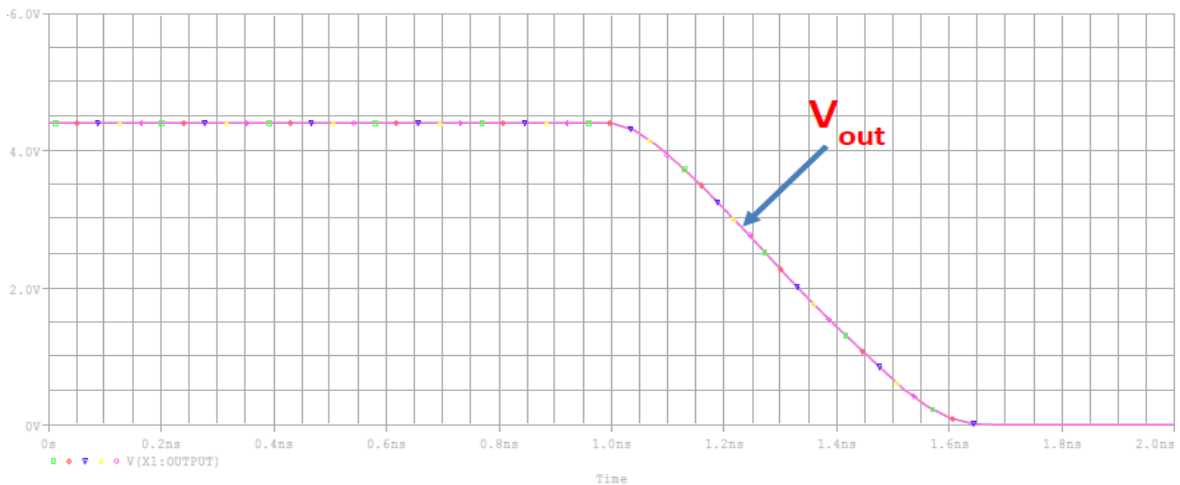
(c)

**Figure 3 (a-c) The inductance swept for the right arm coil geometry.**

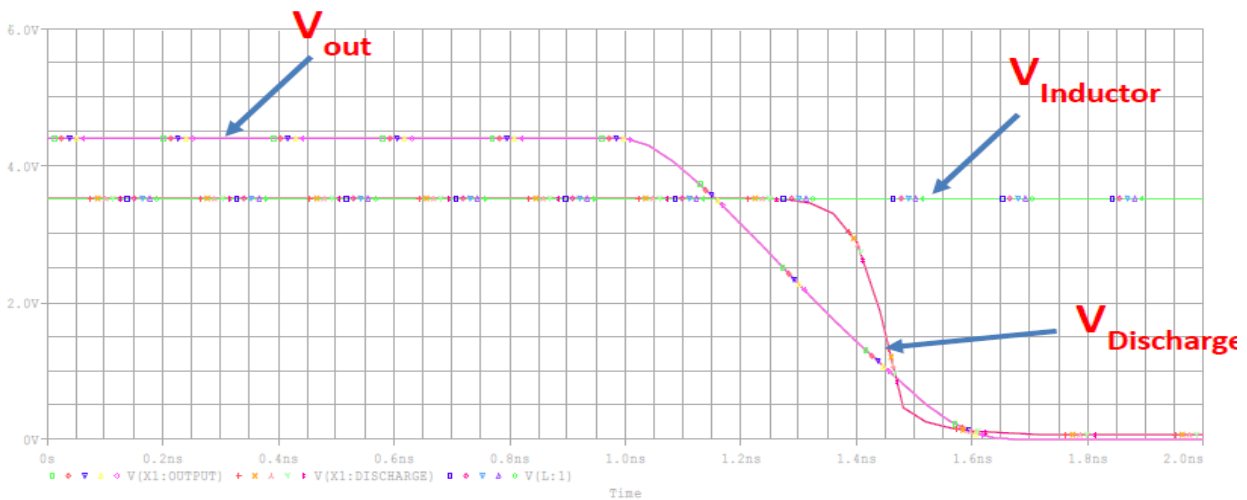
The inductance of the coil two swept also from low to high value is given in Figure 7 (a-c).



(a)



(b)



(c)

Figure 4 (a-c) The inductance swept for the left arm coil geometry

In simulation, we could only vary the inductance value and observe that the  $V_{out}$  is exponentially decreasing at the time interval of  $1\eta s$ - $1.6\eta s$ . As for  $V_{Discharge}$ , it can be seen that the same manner of exponentially decreasing value is observed at the time interval of  $1.3\eta s$ - $1.5\eta s$ . On the other hand, for  $V_{Trigger}$  or  $V_{ind}$ , the voltage remains the same throughout the time interval. From this observation, it can be seen that for both sweeping the parameter of inductance from small to high value and vice versa did not affect the output waveform of the  $V_{out}$ ,  $V_{Discharge}$  and  $V_{ind}$ . Since the  $V_{ind}$  remains constant at certain voltage throughout the time interval, it is difficult to calculate the duty cycle as well as to determine  $T_H$  and  $T_L$  for magnetizing and demagnetizing of the inductor itself. Unlike simulation for only one value of inductor, we can simply determine the  $T_H$  and  $T_L$  for a particular inductance value. With known  $T_H$  and  $T_L$ , we can calculate the frequency and duty cycle (Ferran R. 2009).

Tables 1 and 2 show the inductance values swept for the right arm coil and the left arm coils.

**Table 1 The inductance value swept for the right arm coil**

Step Parameter	Inductance value
L0	500 $\mu H$
L1	1.5mH
L2	2.5mH
L3	3.5mH
L4	4.5mH

**Table 2 The inductance value swept for the second coil**

Step Parameter	Inductance value
L0	5mH
L1	4mH
L2	3mH
L3	2mH
L4	1mH

A linear relationship exists between the inductance of the right arm coil, which increases when the core is moving in, while the core for the left arm coil is moving out, with decrease in inductance. The inductance change is simulated and plotted in Figure 4 (a) and (b). These inductance changes lead to a frequency change and hysteresis for the output of the timers as seen from derivations and simulation results. This shows that the frequency is decreasing when the core is going in and increases when the core goes out. At equilibrium state when the seesaw bar is horizontal, the displacement  $x$  is equal to half of the coil length, and the value of the inductance for both coils is the same (Bruno 2013). This is clearly shown in Figure 4 (a) at the point when  $x= 10mm$ , the inductance  $L=4.67mH$  for the two coils. The result of the inductance equality at this point is reflected to the frequency value as Figure 5 (a) and 5 (b). The main difference between derivations and simulation results is seen when the coil is almost fully out. From derivation point, when the coil is fully out  $x=0$ , the frequency is larger than 800 MHz, which is very large compared to other frequency values which ranges from 0.18 to 3.4 MHz. On the other hand, simulation result shows that maximum frequency occurs when the core is fully out and this is at 3 MHz as shown Figure 5 (a) and 5(b). Although, the result from derivations and simulation has shown that the seesaw bar frequency has no much effect on the output frequency values, the frequency counter calculates the value

which is equal to the time period of the timer output for every reading. So, if the seesaw frequency  $f_s$  exceeds a certain value, the frequency counter will give wrong frequency output.

### 5. SENSOR CIRCUIT LINEARIZATION AND IMPROVEMENT OF SENSITIVITY

The circuit configurations in Figure 8 are simulated using PSpice to observe the process of magnetization and demagnetization of the inductor as in Figure 8(a), as well as charging and discharging of the capacitor shown in Figure 8(b) (Ezzat 2011). The simulation graph is as shown in Figure. 10 (a) and Figure 10 (b) respectively (Ferran 2009 and Ezzat 2011), Deji A., Sheroz K., Musse M.A., (December 2023 and Deji A., Sheroz K., Musse M.A., (December 2023, Zvezditz P. Nenova and Toshko G. N., (February 2009)

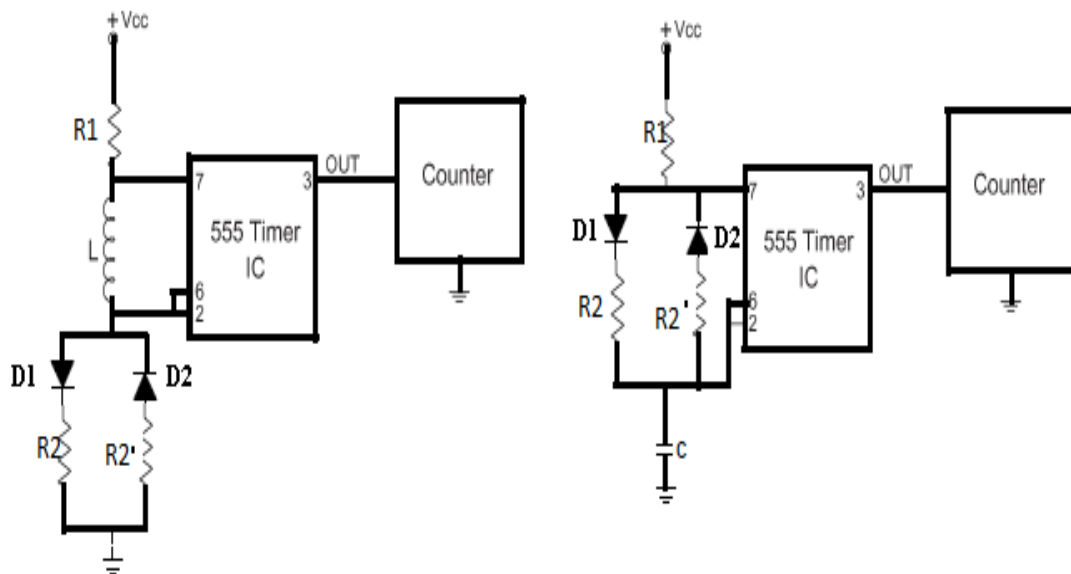


**Figure: 5 Simulation of the circuit for linearization**

The equations for frequency as derived in previously reported work have been modified differentially to compensate for linearity issues leading equation 1, hence showing results in Figure 9.

$$f = \frac{1}{L_{wind} \left( 1 + \frac{x}{l} (\mu_r - 1) \right) \left[ \frac{0.693}{R_2} + \frac{1}{R_1 + R_2} \ln \left( \frac{2R_1 - R_2}{R_1 - 2R_2} \right) \right]} \quad (1)$$

$$f = \frac{1.44}{C(R_1 + 2R_2)} \quad (2)$$

The plot for the frequency variation with respect to the displacement  $x$  is shown in Figure 9. Only the plot from the right arm coil is presented here. Although the variation of frequency is affected by the variation of displacement and its applicable to both inductors and capacitors. The search is focused more towards the inductive sweeping and changes. It can be seen that the frequency keeps on decreasing as the displacement  $x$  of core insertion into the coil is increasing (Ezzat 2011).

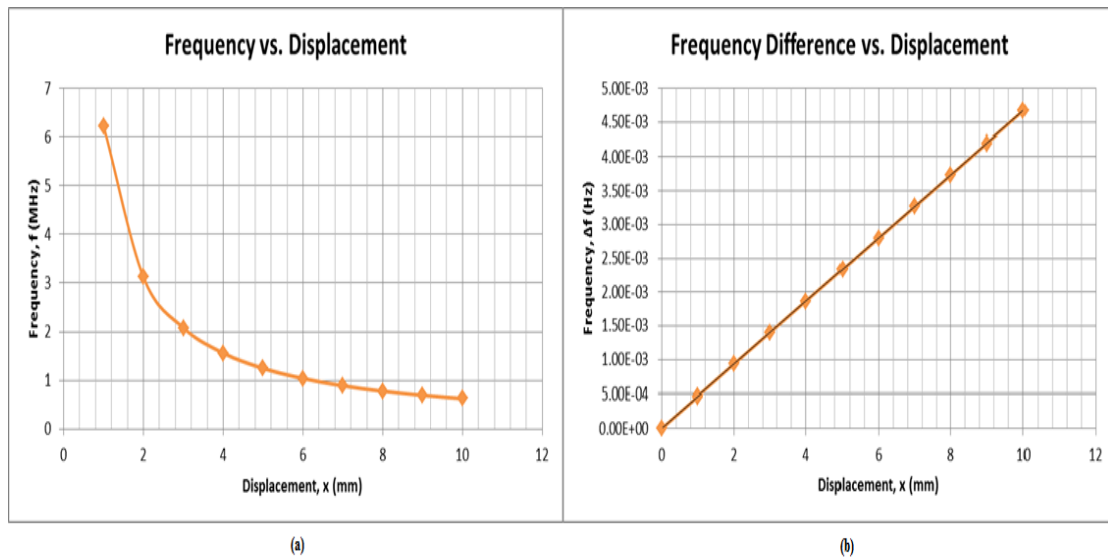


**Figure 6 (a) Variation of frequency with displacement, (b) Variation of differential frequency with displacement.**

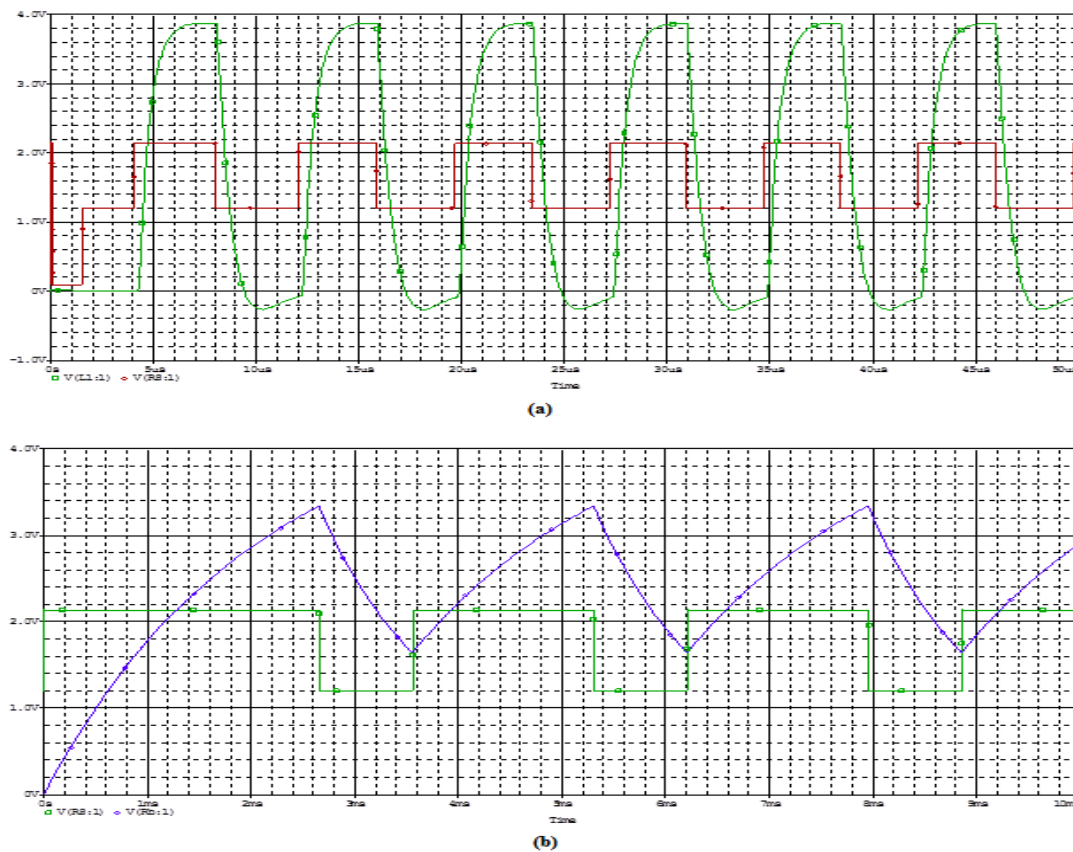


**Figure :7 Simulation of the position sensor circuit with diode for linearization**

From this research, it is discovered that the IC 555 timer has various application. It can be used as a normal timer, or it's used as an oscillator in a circuit that converts the unknown capacitance and inductance to frequency variations. The duty cycle is given by

$$\% DC = \frac{t_H}{t_H+t_L} = \frac{t_H}{T} \% \quad (3)$$

By adding the diodes in the circuit configuration, as in Figure 8, the duty cycle of the circuit are improved, where the difference between  $R_1$  and  $R_2$ , as well as  $R_2$ , are relatively low, hence reducing the linearity issue. Moreover, the sensitivity of the sensor is also increased.

From the derivations and plots, it can be seen that the movement of the core, either into or out of the coil, is responsible for the variations of frequency and the frequency difference. The variation of frequency difference with respect to the depth, i.e. displacement  $x$ , is observed through the plots obtained. Based on the derivation and plots obtained, it can be said that the frequency difference in the circuits shown above and are the same. For the circuit configuration of Figure 8, the plot of frequency difference is shown in Figure 9 and is linear. A similar plot is obtained for the frequency difference of the circuit configuration. This shows how sensitive the system is when the cores are inserted or pulled out from the coil at the same time.

## 5.1. MAGNETIZATION AND DEMAGNETIZATION OF RL3R-BASED TIMER CIRCUIT CONCEPT

When the differential circuit is magnetized, the following results are sub sectioned

### 5.1.1. Magnetization:

- Assume inductor L is not magnetized and the voltage across 3R is less than  $1/3V_{CC}$ , then the output of Comparator 2 (S) is HIGH and the output of the Comparator 1 (R) is LOW. Since Q is HIGH, the transistor is turned off and L gets magnetized through R and 3R as it shown in Figure 11
- When the voltage across 3R reaches  $1/3V_{CC}$ , the output of Comparator 2 changes to LOW (S=0 & R=0), and L continues getting magnetized.
- L continues getting magnetized until it reaches  $2/3V_{CC}$ . At this point, the comparator 1 changes to a HIGH state (S=0 & R=1), the output Q of the SR flip-flop goes to LOW.

### 5.1.2. Demagnetization

- The HIGH output of flip-flop ( $Q^{\wedge}$ ) turns ON the transistor, which creates a demagnetizing path through 3R as it shown in Figure 11), then the output of Comparator 1 changes to LOW (S=0 & R=0), and L continues getting demagnetized.
- When the voltage across the 3R reaches  $1/3V_{CC}$ , comparator 2 output changes to HIGH and the flip-flop output turns off the transistor and L begins to get magnetized again.

The waveform for the circuit in Figure 11. A Pspice program was used to simulate this circuit and to get the wave form. The green line is the 3R resistor current, and the red one is the output voltage from the sensor as shown in Figure 11.

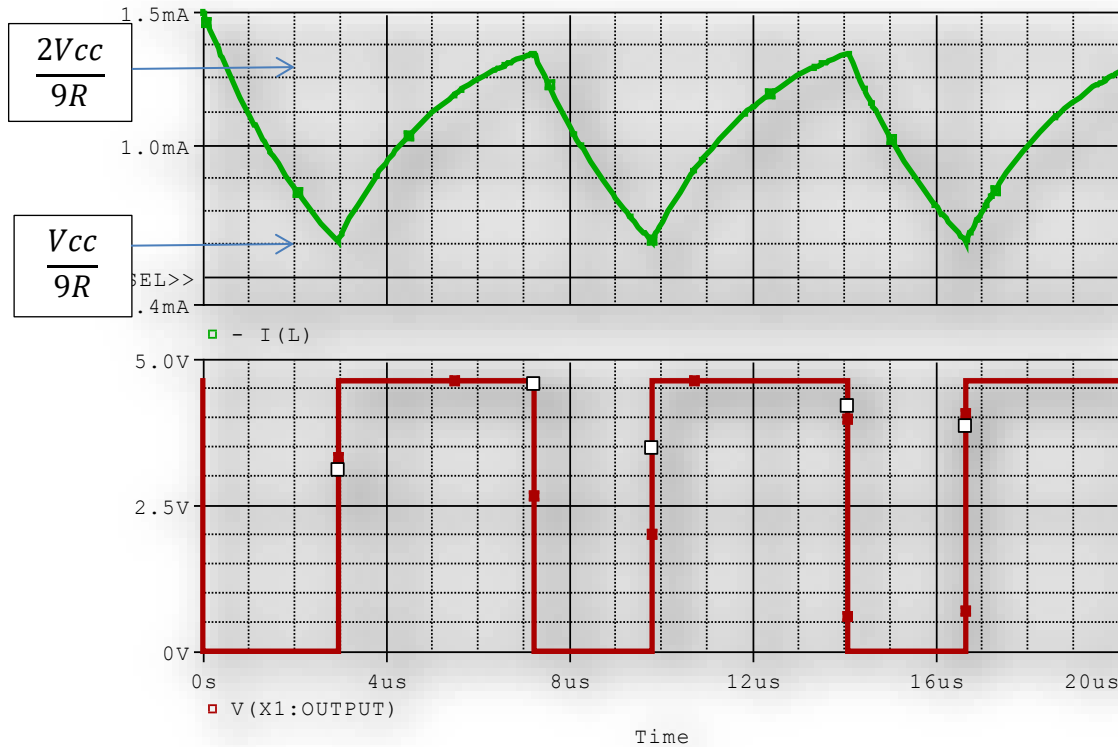


**Figure: 8 Current and voltage waveform from the position**

It's noticed that while L is getting magnetized, the output of the 555 timer is HIGH; while it's demagnetizing, the output of the 555 timer is LOW,  $t_h$  is depending on R and L values and given.

## 5.2.CHARGING AND DISCHARGING THROUGH $R_1R_2C$ -BASED TIMER CIRCUIT

The charging characteristic of the RRC based circuit is shown in subsection below

### 5.2.1. Charging characteristics through RRC:

- Assume the voltage across  $C_1$  is less than  $1/3V_{CC}$ , then the output of comparator 2 (S) is HIGH and the output of the comparator 1 (R) is LOW. Since Q is HIGH, the transistor is turned off and  $C_1$  begins charging through  $R_1$  and  $R_2$  as shown. When the voltage across  $R_2$  reaches  $1/3V_{CC}$ , the output of Comparator 2 changes to LOW ( $S=0$  &  $R=0$ ), and  $C_1$  continues charging.
- $C_1$  continues charging until it reaches  $2/3V_{CC}$ . At this point, the comparator 1 changes to a HIGH state ( $S=0$  &  $R=1$ ), the output Q of the SR flip-flop goes to LOW.

### 5.2.2. Discharging characteristics through RRC:

- The HIGH output of flip-flop ( $Q'$ ) turns ON the transistor which creates a discharging path through  $R_2$  as it shown, then the output of comparator 1 changes to LOW ( $S=0$  &  $R=0$ ), and L continues discharging.
- When the voltage across the  $R_2$  reaches  $1/3 V_{CC}$ , Comparator 2 output changes to HIGH and the flip-flop output turns off the transistor and  $C_1$  begins charging again.

Figure 12 is the waveform obtained from  $R_1R_2C$  simulation using Pspice. The red line is the capacitor voltage and the green line is the output voltage from the sensor. This graph thus shows that C is charging from  $V_{cc}/3$  to reach  $2/3V_{cc}$ , and discharging from  $2/3 V_{cc}$  to  $V_{cc}/3$ .



**Figure: 9 The capacitive and output voltage from the sensor**

While the C1 is charging, the output of the 555 timer is HIGH; while it's discharging, the output of the 555 timer is LOW as shown in Figure 12.

## 6. Conclusion

This research article explores the utility of the seesaw model sensor apparently giving a differential output in a differential manner, which validates one of the major findings of this research. In this article, simulation is carried out of the designed mathematical model and its necessary derivations for frequency, frequency hysteresis, sensing voltage, magnetic field strength, resonant frequency, mass of bar and mass of target object and the current excitation responses sweeping voltages, charging/discharging current magnetization and demagnetization are obtained. Furthermore, the linearity issues of the transducer response curve are addressed for an application scenario of using an inductor with 3R resistor in a differential manner. The parameter of interest is displacement of the core bringing about changes in inductance. Displacement makes the differential inductor to oscillate and undergo changes in differential style. Other parameters of interest such range, frequency, inward output voltage, outward output voltage. This circuit has been applied to a servo machine harvesting the oscillation/vibration into inductance and frequency and voltage output. The simulated sensor has also been tested for managing imaging signal for biomedical signal acquisition.

## Acknowledgement

The authors will like to thank the Research Management Center of Waidsum University.

## References

1. Deji, A., Khan, S., Habaebi, H.M., Musa. O.S. (2024). Technical Engineering Evaluations and Economic Feasibility Study of Solar Powered Air Conditioning System in Tier Three Nations. *Academy of Entrepreneurship Journal*, 30(S1), 1-18.
2. Deji A., , Sheroz K., Musse M.A., (Jan-Feb 2024). Experimentation and Application of Differential Inductive System for Machine and Human body parametric Measurement. *International Journal for Multidisciplinary Research (IJFMR)*. Volume 6, Issues 1, January-February 2024, Page 1-19. <https://doi.org/10.36948/ijfmr.2024.v06i01.11787>.
3. Deji A., Sheroz K., Musse M.A., (December 2023) “Analytical Modeling of Electrical Frequency and Voltage Signal from a Differential Inductive Transduction for Energy Measurement. *International Journal for Multidisciplinary Research*. Volume 5 Issue 6 Page 1-19. DOI: [10.36948/ijfmr.2023.v05i06.8292](https://doi.org/10.36948/ijfmr.2023.v05i06.8292)
4. Deji A., Sheroz K., Musse M.A., (December 2023) “Kinematic Motion Modelling from Differential Inductive Oscillation Sensing for a Sevomechanism and Electromechanical Devices and Applications. *International Journal for Multidisciplinary Research*. Volume 5 Issue 6 Page 1-15. DOI: [10.36948/ijfmr.2023.v05i06.8291](https://doi.org/10.36948/ijfmr.2023.v05i06.8291)
5. Deji A., Hanifah A.M., Sherifah O.M., (December 2023) “The Adoption of Information System Technology in Piloting the Current State of Health Institution in Tier Three Nations.” *International Journal for Multidisciplinary Research*. Volume 5 Issue 6 Page 1-13. DOI: [10.36948/ijfmr.2023.v05i06.8367](https://doi.org/10.36948/ijfmr.2023.v05i06.8367)
6. Mohammed, S.S., B. George and L. Vanajakshi, 2012. “A Multiple Inductive Loop Vehicle Detection System for Heterogeneous and Lane-Less Traffic,” *IEEE Transactions On Instrumentation and Measurement*,61(5): 1353-1361.
7. Ezzat, G.B. and H.M. Marvin Cheng, AUGUST 2011. “High-Sensitivity Inductive Pressure Sensor,” *IEEE Transactions On Instrumentation And Measurement*, 60(8).
8. Zvezditz P. Nenova and Toshko G. N., (February 2009). Linearization Circuit of the Thermistor Connection. *IEEE Trans. on Instrumentation and Measurement*, Vol.58, No.2: 441-449.
9. D. Abdulwahab et al., "Identification of linearized regions of non-linear transducers responses," International Conference on Computer and Communication Engineering (ICCCE'10), Kuala Lumpur, 2010, pp. 1-4, doi: 10.1109/ICCCE.2010.5556753.
10. Ferran R. and Oscar C., (October 2009). Interfacing Differential Resistive Sensor to Microcontrollers: A Direct Approach. *IEEE Trans. on Instrumentation and Measurement*, Vol.58, No.10: 3405-3410.
11. D. Abdulwahab, S. Khan, J. Chebil and A. H. M. Z. Alam, "Symmetrical analysis and evaluation of Differential Resistive Sensor output with GSM/GPRS network," 2011 4th International Conference on Mechatronics (ICOM), Kuala Lumpur, Malaysia, 2011, pp. 1-6, doi: 10.1109/ICOM.2011.5937149.
12. Khan S., A. Deji, A.H.M Zahirul, J. Chebil, M.M Shobani, A.M Noreha. (Setember 2012) “Design of a Differential Sensor Circuit for Biomedical Implant Applications”. *Australia. Journal of Basic and Applied. Sciences.*, 6(9): 1-9. [10.1002/9781118329481.ch1](https://doi.org/10.1002/9781118329481.ch1).
13. Deji A., Sheroz K, Musse M.A, Jalel C. (August 2014). Analysis and evaluation of differential inductive transducers for transforming physical parameters into usable output frequency signal August 2014 [International Journal of the Physical Sciences](https://doi.org/10.5897/IJPS12.655) 9(15):339-349. DOI:[10.5897/IJPS12.655](https://doi.org/10.5897/IJPS12.655)

14. Deji A., Sheroz K, Musse M.A, Jalel C. (2011). Design of Differential Resistive Measuring System and its applications. A book chapter in IIUMPRESS on Principle of Transducer Devices and Components. Chapter 17, page 107.
15. Abdulwahab, Deji. *Development of Differential Sensor Interface for GSM Communication*. Kulliyyah of Engineering, International Islamic University Malaysia, 2011.
16. Abdulwahab Deji. *Development of Differential Inductive Transducer System for Accurate Position Measurement*. Kulliyyah of Engineering, International Islamic University Malaysia, 2016 Practical EE Copyright 2019). [www.eepractical.com](http://www.eepractical.com)
17. Deji A., Sherifah OM., 2023. *The Mediating Effect of Entrepreneur Cash Waqf Intension as means of Planned Behaviour for Business Growth. International Journal for Multidisciplinary Research. Volume 5, Issues 6, page 1-22*
18. Elfaki Ahamed, O.M.H., Musa O.S, Deji A., (2023). Factors Related to Financial Stress Among Muslim Students in Malaysia: A Case Study of Sudanese Students. *Academy of Entrepreneurship Journal*, 29(6), 1- 15.